GRID-BASED SOIL-WATER EROSION AND DEPOSITION MODELING USING GIS AND RS

Seong-Joon Kim

Department of Agricultural Engineering, Konkuk University, Seoul 143-701, Korea

Abstract: A grid-based KIneMatic wave soil-water EROsion and deposition Model (KIMEROM) that predicts temporal variation and spatial distribution of sediment transport in a watershed was developed. This model uses ASCII-formatted map data supported from the regular gridded map of GRASS (U.S. Army CERL, 1993)-GIS (Geographic Information Systems), and generates the distributed results by ASCII-formatted map data. For hydrologic process, the kinematic wave equation and Darcy equation were used to simulate surface and subsurface flow, respectively (Kim, 1998; Kim et al., 1998). For soil erosion process, the physically-based soil erosion concept by Rose and Hairsine (1988) was used to simulate soil-water erosion and deposition. The model adopts single overland flowpath algorithm and simulates surface and subsurface water depth, and sediment concentration at each grid element for a given time increment. The model was tested to a 162.3 km^2 watershed located in the tideland reclaimed area of South Korea. After the hydrologic calibration for two storm events in 1999, the results of sediment transport were presented for the same storm events. The results of temporal variation and spatial distribution of overland flow and sediment areas are shown using GRASS.

Key Words: Grid-based, Soil-water erosion, GRASS, GIS, Remote Sensing

1. INTRODUCTION

Erosion prediction is the most widely used and most effective tool for soil conservation planning and design. The loss of soil due to surface runoff as well as the pollution in runoff, seepage or percolation from agricultural management activities is one of the major problems in modern agricultural management. Modeling soil erosion is the process of mathematically describing soil particle detachment, transport and deposition on land surfaces. Erosion model can be used as predictive tools for assessing soil loss for conservation planning, project planning, soil erosion inventories and for regulation. The soil loss equation such as developed by Rose et al. (1983a,b) should equally apply independent of the mechanism that determines the runoff as long as the quantity and velocity of the water flow is predicted correctly.

A factor-based soil erosion model is not suitable for extrapolation beyond the limits of the data set. A physically-based model of soil erosion processes has the capacity to extrapolate and generalize beyond the database used to check its utility (Rose, 1993). It also can simulate sediment movement accurately with little or no calibration of parameters (Bingner, 1990). Physically-based mathematical models can predict where and when erosion is occurring, thus

helping the conservation planner target efforts to reduce erosion. A mathematical concept of soil-water erosion and deposition developed by Rose et al. (1983a) was adopted in this study. It represents mathematically the rates of rainfall detachment, sediment deposition, and soil entrainment by overland flow. It uses the concept of stream power in representing the entrainment processes. It expresses the conservation of mass of sediment to an ordinary differential equation, which can be solved analytically. The solution gives sediment concentration at any time as a function of distance down the plane. Geographic Information Systems can provide a practical solution for handling the detailed spatial variability within a watershed. GIS also can preserve the spatially oriented data structures and operations to maintain the physical meaning at any point in the modeling process (Zollweg, 1994).

The objective is to develop an event-based soil erosion model in areas where the Hortonian overland flow is the mechanism that generates runoff. A grid-based soil-water erosion and deposition procedure is described. This approach predicts the temporal variations and spatial distributions of sediment transport areas and their concentrations during a storm event. The model coded in UNIX-C language runs on the GRASS and uses regular gridded data such as elevation, stream, land use and soil information. The results are displayed on GRASS.

2. MODEL DESCRIPTION

2.1 Grid-based water balance components

The schematic representation of water balance components in a grid element is shown in Figure 1.

2.2 Surface runoff

The kinematic wave equation for overland/stream flow are obtained by the Manning equation:

$$Q = \alpha R^{m1} A^{m2} \quad (1)$$

where Q = discharge (m^3/sec); $\alpha = n^{-1} W^{-2/3} \tan^{1/2}\beta$ for overland flow, $n^{-1} \tan^{1/2}\beta$ for stream

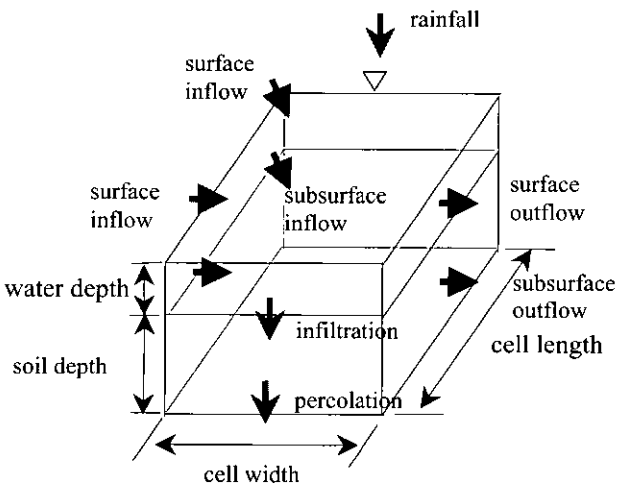

Figure 1. Grid-based water balance components

flow; n = Manning's roughness coefficient; W = grid element width orthogonal to streamline (m), β = grid element slope (degree), R = H for overland flow (m), γ A $^{1/2}$ for stream flow; H = flow depth (m); γ = 0.354 for rectangular channel (Moore and Foster, 1990; Moore and Burch, 1986); A = cross sectional flow area (m^2); m1 = 0 for overland flow, 2/3 for stream flow; m2= 5/3 for overland flow, 1.0 for stream flow.

2.3 Subsurface runoff

Lateral saturated subsurface flow equation approximated by the kinematic assumption (Beven, 1982; Sloan and Moore, 1984) was adopted:

$$Q_{sub} = K_s A \sin\beta \quad (2)$$

where Q_{sub} = subsurface discharge; K_s = saturated hydraulic conductivity (m/sec).

2.4 Infiltration and Percolation

Huggins and Monke infiltration equation (Beasley, et al., 1980) was adopted, and the percolation rate was applied when the soil moisture is over the field capacity.

$$f = f_c + f_i (SM_r / PO_e)^b \quad (3)$$

where f = infiltration rate (mm/hr); f_c = final infiltration rate (mm/hr); f_i = initial infiltration rate (mm/hr); SM_r = available storage capacity (m^3/ m^3); PO_e = effective porosity (m^3/m^3); b = constant coefficient.

2.5 Initial flow depth condition

The spatial distribution of initial subsurface flow depths in a watershed can be obtained from soil information maps describing porosity, field capacity and initial soil moisture conditions. The initial flow depth for each grid element can be calculated by

$$\begin{aligned} H_i &= D_c (SM_i - F_c) /(PO_e - F_c), && F_c < SM_i < PO_e \\ &= D_c, && SM_i \geq PO_e \\ &= 0, && SM_i \leq F_c \end{aligned} \quad (4)$$

where H_i = initial flow depth in grid element (m); D_c = soil depth above the impeding layer (m); SM_i = initial soil moisture content (m^3/m^3); F_c = field capacity (m^3/m^3).

2.6 Grid-based water balance calculation

Water balance in a grid element is sequentially calculated beginning from the most upper left grid element to the lowest right grid element. The calculated outflow delivered to the neighbor grid element by flow direction is stored and used as inflows of the grid element at the next time step. The water balance equation for overland flow and stream flow is,

$$\frac{dSi}{dt} = P(t)i - F(t)i + \sum Q_{in.i} - Q_{out.i}$$

for overland flow

$$\frac{dSi}{dt} = P(t)i - F(t)i + \sum Q_{in.i} + \sum Q_{sub.in.i} - Q_{out.i}$$

for stream flow (5)

where i = grid element address; S_i = grid element storage (m^3); P_i = rainfall (m^3/sec); F_i = infiltration (m^3), $Q_{in.i}$ = inflows to the grid element (m^3/sec); $Q_{out.i}$ = outflow from the grid element (m^3/sec); $Q_{sub.in.i}$ = subsurface inflows to the grid element (m^3/sec); t = time (sec).

The soil moisture routing equation is,

$$\frac{dSMi}{dt} = F(t)i + \sum Q_{sub.in.i} - Q_{sub.out.i} - DP(t)_i \quad (6)$$

where SM_i = soil moisture content in the grid element (m^3); $Q_{sub.out.i}$ = subsurface outflow from the grid element (m^3/sec); DP_i = Deep percolation to the groundwater (m^3).

2.7 Soil-water erosion and deposition

The source of power available from the flow to either entrain or reentrain sediment is the rate of working of the shear stress called the "stream power" (Ω) by Bagnold (1977). The stream power using the kinematic approximation for the mean shear stress per unit area of wetted surface is given by,

$$\Omega = \rho g S R_h V \tag{7}$$

where Ω = stream power (W/m^2), ρ = water density (kg/m^3), g = gravitational constant (m/sec^2), S = grid element slope (m/m), R_h = hydraulic radius (m), V = mean velocity (m/sec).

2.7.1 Sheet flow

A portion of the stream power is effective in increasing the concentration of sediment in overland flow by the processes of entrainment and re entrainment. The upper concentration limit of sediment, called the transport limit by Foster (1982), is shown by Hairsine and Rose (1992a) to be given for sheet flow over a bare surface by,

$$c_t = \frac{F\rho}{\phi}\left(\frac{\sigma}{\sigma-\rho}\right)SV \tag{8}$$

where c_t = the upper concentration limit (kg/m^3), F = the fraction of stream power effective in erosion, σ = sediment density (kg/m^3), ϕ = sediment depositability (m/sec).

The sediment depositability is shown by Rose et al. (1990) to be,

$$\phi = \sum_{i=1}^{I} v_i / I \tag{9}$$

where v_i = sediment settling velocity of the particle class (m/sec), i = particle size class, I = the number of different particle size classes.

The transport limit c_t indicates maximum concentration when the soil surface is completely covered by a deposited layer. Rose (1993) presented a method for relating the actual concentration c to the transport limit c_t by

$$\bar{c} = \bar{c}_t^{\eta} \tag{10}$$

where $\bar{c}$ = the mean sediment concentration during the erosion event, $\bar{c}_t$ = the mean value of the sediment concentration at the transport limit, η = the erodibility parameter ($0 \le \eta \le 1$).

In this study, η is ascribed one value where erosion is predicted and the sediment concentration tends to approach the transport limit, and another lower value where deposition is predicted and the sediment concentration is significantly below the transport limit.

2.7.2 Rill flow

In case of rill flow, we can assume that the grid surface contains N rills per unit width, and all rills are parallel and at the slope of grid element. Assuming rectangular rills of width W_r (m) and water flow depth H (m), the transport limit c_t is given by (Hairsine and Rose, 1992b),

$$c_t = \frac{F}{\phi}\left(\frac{\sigma}{\sigma-\rho}\right)\frac{\Omega}{gH}\left(\frac{W_r}{W_r+2H}\right) \tag{11}$$

where W_r = rill width (m).

2.7.3 Vegetation flow

Hairsine and Rose (1992a) described the situation where entrainment and reentrainment

act together, assuming the layer of deposited sediment covers some fraction H_{ds} of the soil surface. The expression for the rate of entrainment of particles of any general size class i is,

$$r_i = (1 - H_{ds})\frac{F\Omega}{IJ}(1 - C_g) \tag{12}$$

where r_i = the rate of entrainment of size class I ($kg/m^2/sec$), H_{ds} = the deposited sediment fraction, J = the specific energy of entrainment of the soil (J/kg), C_g = the fraction of potential contact cover ($0 \le C_g \le 1$).

The expression for reentrainment of size class i is (Hairsine and Rose, 1992a),

$$r_{ri} = \frac{\delta_i H_{ds} F\Omega}{gH}\left(\frac{\sigma}{\sigma - \rho}\right)\frac{v_i}{\sum_{i=1}^{I} v_i}(1 - C_g) \tag{13}$$

where r_{ri} = the rate of reentrainment of size class i ($kg/m^2/sec$), δ_i = a nonuniform vertical distribution of sediment.

Siepel (1994) expressed the proportion of shear stress on bare soil as a nonlinear function of uncovered portion of the soil surface by the following relationship,

$$\frac{\tau_{ss}}{\tau_s} = (1 - C_g)^{\varepsilon} \tag{14}$$

where τ_s = the total shear stress (N/m^2), τ_{ss} = the shear stress on the bare soil (N/m^2), ε = model parameter. Then the shear stress on the bare soil τ_{ss} is,

$$\tau_{ss} = \rho gSHV(1 - C_g)^{\varepsilon} \tag{15}$$

and consequently the stream power is given by,

$$\dot{U} = \tau_{ss} V = \rho gSHV(1 - C_g)^{\varepsilon} \tag{16}$$

The overland flow per unit width as a function of ℓ is given by,

$$q(\ell) = q_o + R\ell \tag{17}$$

where q = the discharge of grid element per unit width (m^2/sec), q_o = overland flow at the inlet of grid element ($\ell = 0$), R = rainfall intensity (m/sec). The velocity of sheet flow over the vegetated surface can be estimated solving Manning's equation for H in terms of V yields,

$$H = R_h = \left(\frac{Vn}{S^{1/2}}\right)^{3/2} \tag{18}$$

The continuity equation for the unit width of sheet flow gives,

$$V = \frac{S^{0.3}}{n^{0.6}} q(\ell)^{0.4} \tag{19}$$

At some relatively small value of ℓ, call it $\ell = \ell_o$, the sediment concentration will reach a minimum(c_{min}). Thus he assumed that the rate of reentrainment equals the rate of deposition if the distance from the inlet of grid element is far enough ($\ell > \ell_o$). This assumption is reasonable because the sum of the rates of entrainment and reentrainment exceeds the rate of deposition, and reentrainment occurs more rapidly than entrainment.

An expression for H_{ds} can be obtained by setting the rate of reentrainment equal to the rate of deposition, that is $r_{ri} = d_i$, where, d_i is given by $d_i = \delta_i v_i c_i$. Summing over all I size classes, and solving for H_{ds} yields,

$$H_{ds} = \frac{gcH\phi}{F\Omega(1-C_g)}\left(\frac{\sigma-\rho}{\sigma}\right) \quad (20)$$

The change in sediment flux is given by the equation for sediment conservation $dq_{si}/d\ell = r_i + r_{ri} - d_i$. Substituting Eqs. 12, 16, 19 and 20 for r_i, summing over all I size classes, and noting that $q_{si} = qc_i$ where q is the discharge of grid element per unit width,

$$\frac{dc}{d\ell}q(\ell) + c\left[R + \frac{Hg\phi}{J}\left(\frac{\sigma-\rho}{\sigma}\right)\right] = \frac{F\rho gHS^{1.3}}{Jn^{0.6}q(\ell)^{0.4}(1-C_g)^{\varepsilon+1}} \quad (21)$$

which has the following analytical solution,

$$c = \frac{F\rho S^{1.3}}{n^{0.6}\left[1.4\frac{JR}{Hg} + \phi\left(\frac{\sigma-\rho}{\sigma}\right)\right](1-C_g)^{\varepsilon+1}}\left[q(\ell)^{0.4} - q(\ell_o)^{0.4}\right] + c_{min} \quad (22)$$

where c_{min} = sediment concentration at $\ell = \ell_o$ (kg/m^3).

The sediment routing equation for overland flow and stream flow is,

$$\frac{dci}{dt} = \sum(c \bullet Q_{in.i}) - (c \bullet Q_{out.i}) \quad (23)$$

2.8 Model structure and implementation

A schematic flow diagram of the model is shown in Figure 2. As input data of the model, six GRASS regular gridded maps; elevation, stream, flow direction, land use, soil, Thiessen network were prepared. They are converted into ASCII-formatted map data using GRASS command r.out.ascii. The model uses these data to generate flow depth, discharge, sediment concentration and flux at each grid element outlet for a given time interval. In this study, the calculation time step was one minute. Stream flow and sediment concentration at the watershed outlet and ASCII-formatted flow velocity maps,

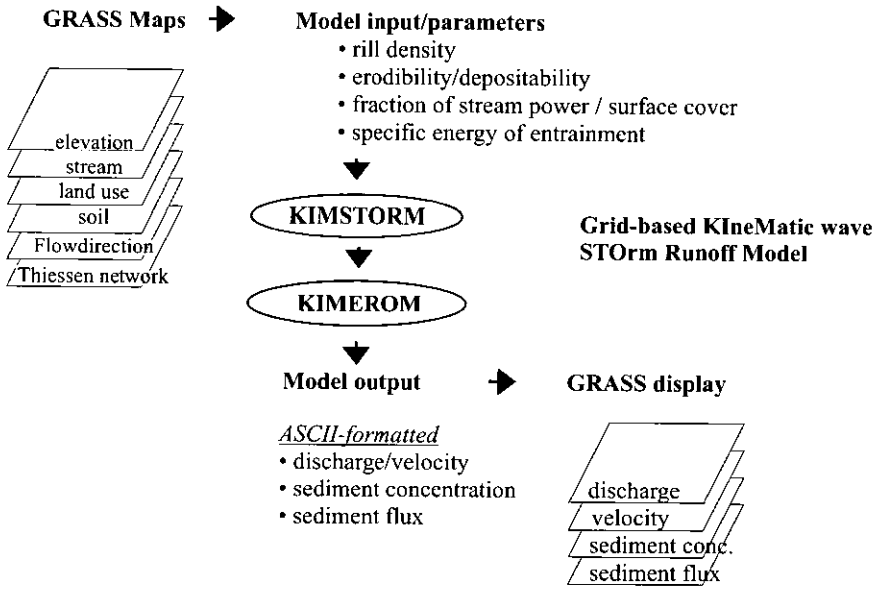

Figure 2. Schematic diagram of KIMEROM model

sediment concentration maps, and sediment flux maps were generated for 1-hr interval. The ASCII-formatted map data were converted into the GRASS maps using GRASS command r.in.ascii.

3. MODEL APPLICATION

3.1 Watershed, soils, land use and storm events

The model was tested with the Hwaong tideland reclaimed area located in the upper western part of South Korea. The watershed area is 162.3 km^2 and elevations range from 0 m to 185 m. The 3 arc-second spacing DEM from the Defense of Mapping Agency of United States was used. The DEM has the grid of 270 rows and 328 columns. By using DEM as input data, the stream and flow direction maps were generated with GRASS 'r.watershed' command (Figure 3). The soil map was rasterized from the vector file (1:25,000 scale) supported from the Ministry of Agriculture and Forestry (Figure 4). The watershed soil is classified by 4 textures of which are 10.1% sandy loam, 23.2% silt loam, 15.8% clay loam and 50.9 % clay, respectively. The surface layer of most soils is permeable with soil depths ranged from 50 cm to 150 cm. To obtain the land cover map, Landsat image (April 10, 1996; path 116 / row 34) merged by SPOT panchromatic image (August 24, 1997; path 304 / row 275) for the watershed were used and classified by using maximum likelihood method. The land cover is composed of 44% forest, 28% paddy field almost around the stream, 15% upland crop, 2% settlement and the rest 11%, respectively (Figure 5). Thiessen net-

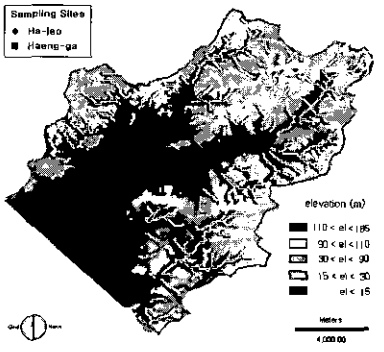

Figure 3. DEM and generated stream map of the study area

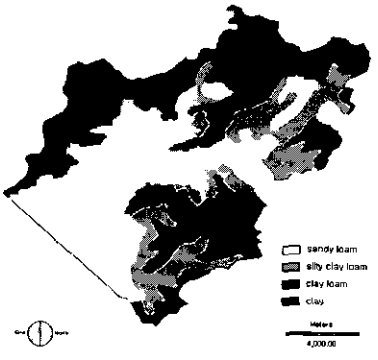

Figure 4. Soil map

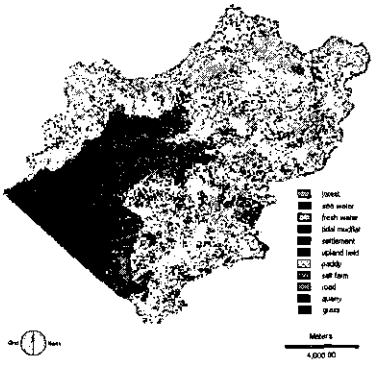

Figure 5. Land cover map

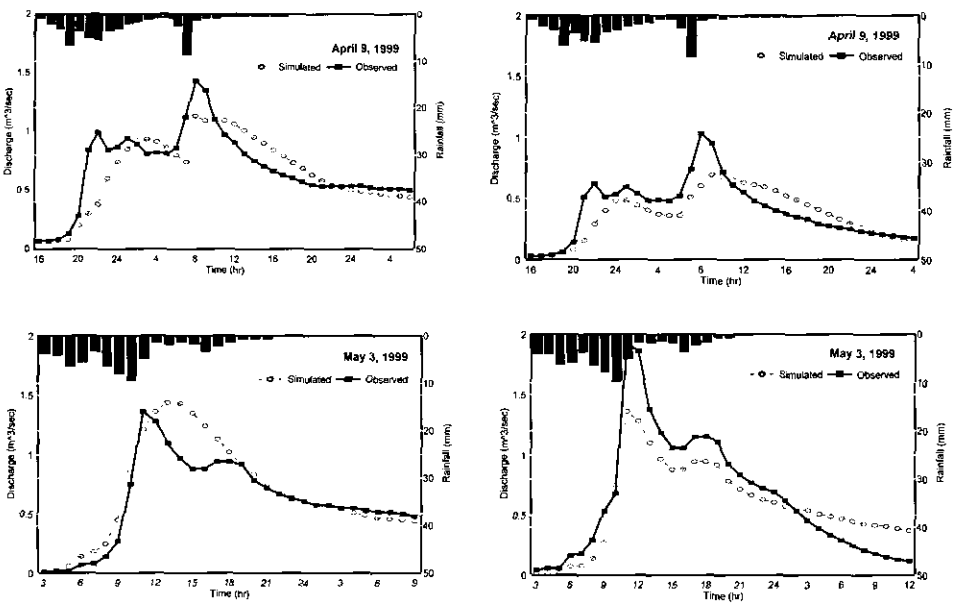

(a) Ha-jeo (b) Haeng-ga

Figure 6. Observed versus predicted stream flow at two locations for April 9 and May 3, 1999

work maps were also rasterized from the valued point vector file. Two storm events (April 9, May 3, 1999) for two locations (Ha-jeo and Haeng-ga) were used for model test. Stream flow data were measured by using auto water level recorders and the suspended solids were sampled with the interval of 1 ~ 4 hours depending on the storm stage.

3.2 Comparing predicted and observed streamflow at two locations

Soil parameters are effective porosity, field capacity and saturated hydraulic conductivity which were adopted from Rawls et al. (1982). In the model calibration, the Manning's roughness coefficients proved to be the most sensitive parameter for overland areas and streams which affected the time and magnitude of the peak stream flow. The next sensitive parameters were the initial and final infiltration rate affecting the magnitude of the peak stream flow. Figure 6 shows the observed versus predicted stream flow at two locations (a: Ha-jeo, b: Haeng-ga marked in Figure 3) for April 9 and May 3 storm. The predicted runoff agreed well with the observed values. Table 1 shows the calibrated parameters and summary for the storm events.

The average Nash-Sutcliffe efficiency R^2 (Nash and Sutcliffe, 1970) for the model was 0.76. The error may be caused by the simplification of subsurface flow. Preferential flow through macro-pores in the soil can contribute to stream flow as a subsurface lateral flow. Other sources of error may arise from the uncertainty of soil depth, initial soil moisture condition and lumping parameters within each grid element.

We cannot determine where the overland flow originated and how much water at each source area contributed knowing only the stream flow at the watershed outlet. Grid-based modeling

Table 1. Parameters used and calibrated for the storm events

Storm event	Total Rain-fall (mm)	Manning's n				Ave. infiltration			Ave.	Total runoff		Peak discharge		Nash-Sutcliffe efficiency
		Stream	Forest	Culti-vated	Settle-ment	f_c (mm/hr)	f_i	b	K_s (m/day)	Obs. (mm)	Pre.	Obs. (m^3/sec)	Pre.	R^2
4/09/99	44.9	0.050	0.38	0.45	0.26	1.9	8.8	0.65	200	6.5	6.3	1.43	1.13	0.80[a]
										5.5	5.0	1.03	0.69	0.61[b]
5/03/99	58.5	0.050	0.28	0.45	0.26	3.0	18.0	0.65	200	4.6	5.1	1.36	1.44	0.79[a]
										8.0	7.3	1.92	1.35	0.82[b]

Note) a: Ha-jeo (14.72 km^2), b: Haeng-ga (9.68 km^2)

approach can also provide information that is important for investigating the loss of soil due to erosion and the transport of non-point source pollutants.

Figure 7 shows the predicted temporal and spatial distribution of saturated overland/stream flow depths for May 3 storm. After the storm started, the overland flow initially occurred around the areas of main stream. These areas have higher soil moisture content than other

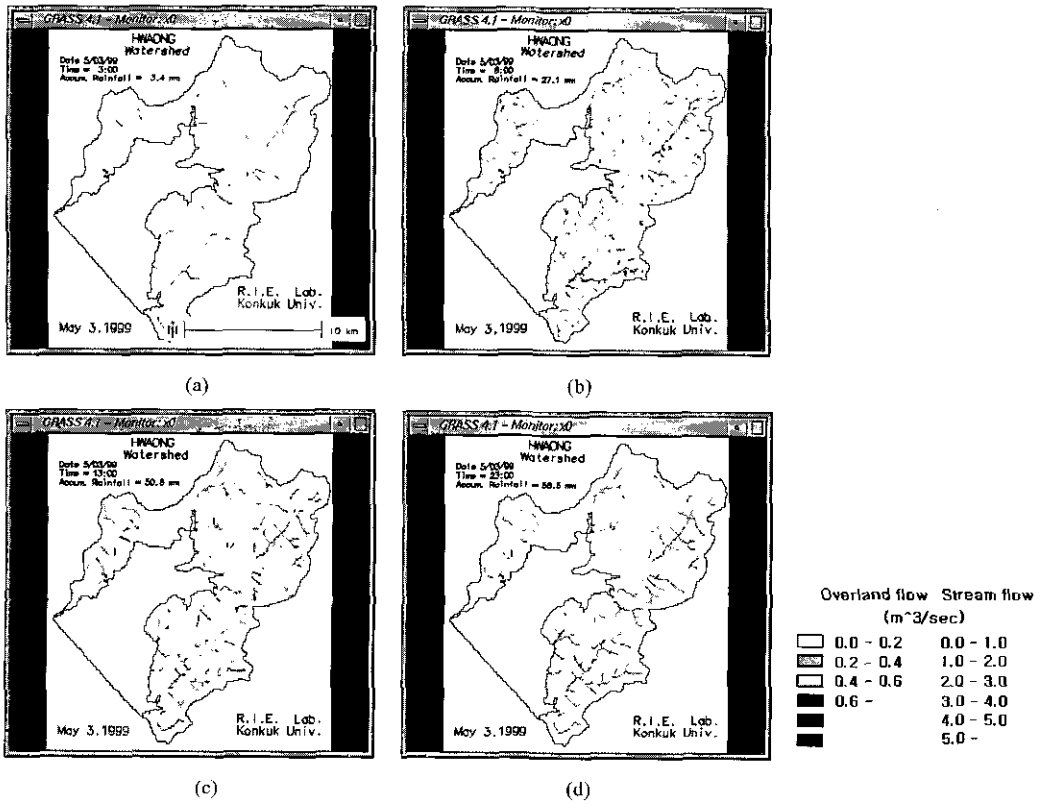

Figure 7. Spatial distribution of surface and channel runoff after (a) 1 hr, (b) 5 hrs, (c) 10 hrs, (d) 20 hrs of rainfall (May 3, 1999)

areas caused by the shallow depth of ground water level, and by the ponding condition of paddy field. The source area for overland flow increased from the start of rainfall to the end of rainfall, and decreased gradually after that time. Also we can find the overland flow areas contributing to stream flows after the peak discharge. This shows that the overland/subsurface flows delayed the transport of water to the watershed outlet causing a lag time.

3.4 Soil-water erosion and deposition simulation

The value of model parameters was adopted from Siepel's study (1994), which was recommended by Rose (personal communication). Detail discussion for parameter sensitivity is found in Kim (1997). Figure 8 shows the observed versus predicted sediment concentration at Ha-jeo watershed outlet for the two storms (April 9 and May 5, 1999). The observed and predicted maximum sediment concentrations for April 9 and May 5 storm were 0.45 kg/m^3, 0.70 kg/m^3 and 0.41 kg/m^3, 0.30 kg/m^3, respectively. The observed and predicted sediment yields for each storm were 14,260.1 kg, 13,020.0 kg and 6,887.8 kg/m^3, 9,785.9 kg/m^3, respectively. The predicted results followed well in accordance with the observed data. The sediment concentration increased in proportion to discharge with some time lag after peak, and then decreased more rapidly in comparison with the decreasing rate of discharge. It was found that sediment depositability (ϕ) and soil erodibility (η) are important to predict sediment discharge. The value ϕ depends on the type of sediment entrained by overland flow. The values used in the model calibration were within the range of those reported for cohesive aggregated soils (0.1 m/sec) by Rose (1993) and for fine sediment (10^{-5} m/sec) by Hairsine and Rose (1992a). Further the values of ϕ showed an increase with increase in stream flow reflecting a change in the type of sediment entrained under different stream flows. The lower values for η were ranged between 0.6 and 0.9 and showed a decrease with increasing stream flow or depositability ϕ.

Temporal and spatial distribution of sediment transport areas by concentration (kg/m^3) for May 3 storm are shown in Figure 9. These distributed results show where the sediment transport originated and how much erosion each source area contributed. Detached soil and the sediment were transported to the stream mostly from the areas that have high overland flow ve-

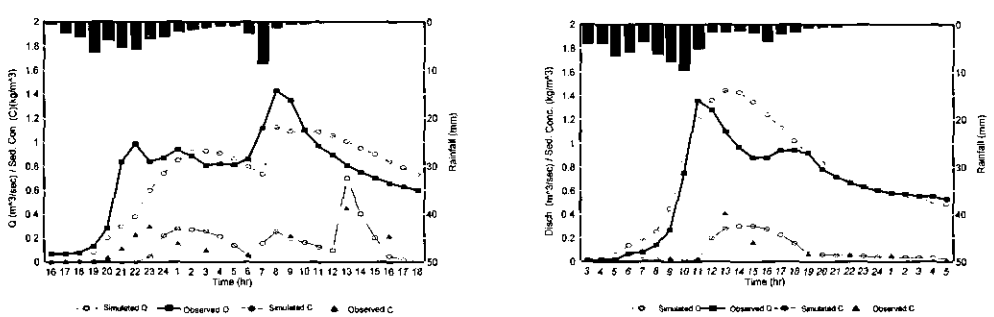

(a) (b)

Figure 8. Observed versus predicted sediment concentration at Ha-jeo watershed outlet ((a) April 9 and (b) May 3, 1999)

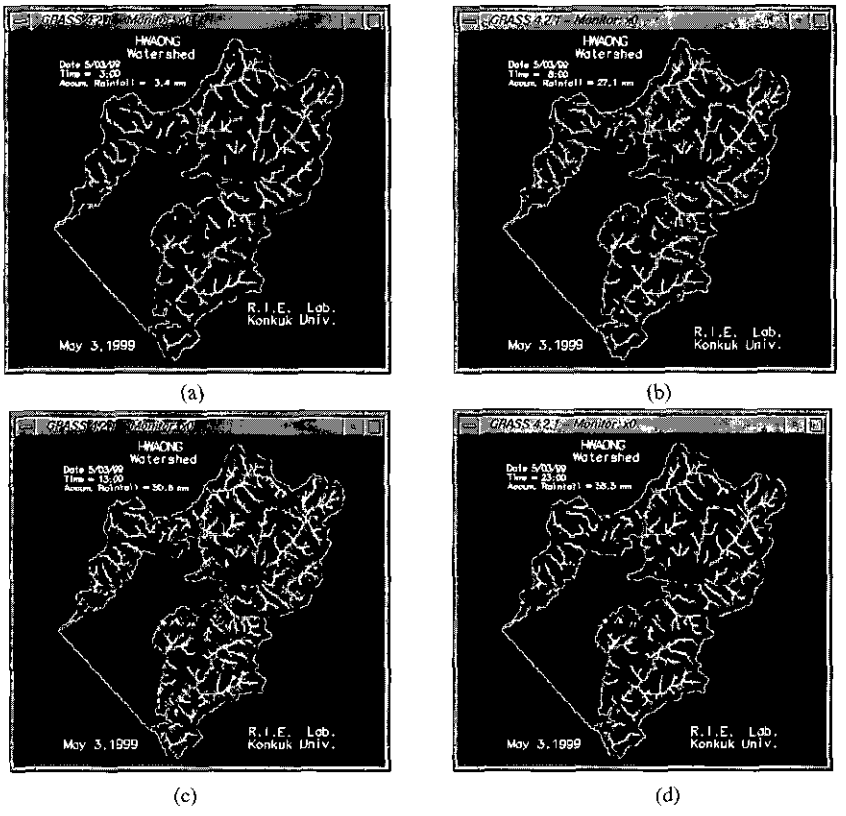

Figure 9. Temporal variation and spatial distribution of sediment transport by concentration after (a) 1 hr, (b) 5 hrs, (c) 10 hrs, (d) 20 hrs of rainfall (May 3, 1999)

locities. This shows that the flow velocity is highly related to the sediment transport. Also it explains that the parameters sediment depositability (ϕ) and soil erodibility (η) are the main factor to control the model behavior.

4. CONCLUSIONS

A grid-based soil-water erosion and deposition model was developed. For hydrologic process, the kinematic wave equation and Darcy equation were used to simulate surface and subsurface flow, respectively. For soil erosion process, the physically-based soil erosion concept by Rose and Hairsine (1988) was used to simulate soil-water erosion and deposition. The model was tested on a 162.3 km^2 watershed located in the tideland reclaimed area of South Korea. As a hydrologic result, the average Nash-Sutcliffe efficiency R^2 (Nash and Sutcliffe, 1970) for the model was 0.76. As a soil erosion result, sediment depositability (ϕ) and soil erodibility (η) were proved as important parameters to predict sediment discharge. The model successfully generated the temporal and spatial distribution of sediment transport areas by concentration and flux, respectively. The distributed results showed that the detached soil and the sediment were transported to the stream from the areas that have high overland flow velocities.

ACKNOWLEDGEMENT

This paper was supported by Konkuk University in 2000.

REFERENCES

Bagnold, R.A. (1977). "Bedload transport by natural rivers." *Water Resour. Res.*, Vol. 13, pp. 303-311.

Beasley, D.B., Huggins, L.F., and Monke, E.J. (1980). "ANSWERS: A model for watershed planning." *Trans. of ASAE*, Vol. 23, No. 4, pp. 938-944.

Beven, K.J. (1982). "On subsurface stormflow: Predictions with simple kinematic theory for saturated and unsaturated flows." *Water Resour. Res.*, Vol. 18, pp. 1627-1633.

Bingner, R.L. (1990). "Comparison of the components used in several sediment yield models." *Trans. of ASAE*, Vol. 33, pp. 1229-1238.

Foster, G.R. (1982). "Modeling the erosion process." In: *Hydrologic modelling of small watersheds*, Hann, C.T. (ed.), Am. Soc. Agr. Eng. Monogr. 5, pp. 297-379, St. Joseph, MI.

Hairsine, P.B. and Rose, C.W. (1992a). "Modeling water erosion due to overland flow using physical principles 1. Sheet flow." *Water Resour. Res.*, Vol. 28, pp. 237-243.

Hairsine, P.B. and Rose, C.W. (1992b). "Modeling water erosion due to overland flow using physical principles 1. Rill flow." *Water Resour. Res.*, Vol. 28, pp. 245-250.

Kim, Seong J. (1997). "Physically-based Soil–Water Erosion Model-based on Hairsine and Rose's Concept." *J. of the Korean Soc. of Agric. Eng.*, Vol. 39, No. 4, pp. 82-89.

Kim, Seong J., Steenhuis, T.S. (1998). "GRId-based variable source area STOrm Runoff Model (GRISTORM)." *Proceedings of the Third International Conference on Hydroinformatics*, A.A. Balkema, Copenhagen, DK, pp. 1383-1390.

Kim, Seong J. (1998). "Grid-based KIneMatic Wave STOrm Runoff Model (KIMSTORM) I. Theory and Model." *J. of Korea Water Res. Assoc.*, Vol. 30, No. 3, pp. 303-308.

Kim, Seong J., Chae, H.S., and Shin, S.C. (1998). "Grid-based KIneMatic Wave STOrm Runoff Model (KIMSTORM), II. Application - applied to Yoncheon Dam watershed." *J. of Korea Water Res. Assoc.*, Vol. 30, No. 3, pp. 309-316.

Moore, I.D. and Burch, G.J. (1986). "Sediment transport capacity of sheet and rill flow: Application of unit stream power theory." *Water Resour. Res.*, Vol. 22, pp. 1350-1360.

Moore, I.D. and Foster G.R. (1990). "Hydraulics and overland flow." In: *Process Studies in Hillslope Hydrology*, Anderson M.G., Burt T.P. (ed), John Wiley, New York, pp. 215-254.

Nash, J.E. and Sutcliffe, J.V. (1970). "River flow forecasting through conceptual models, Part I - A discussion of principles." *J. of Hydrology*, Vol. 10, pp. 283-290.

Rawls, W.J., Brakensiek, D.L. and Saxton, K.E. (1982). "Estimation of soil water properties." *Trans. of ASAE*, Vol. 25, pp. 1316-1320.

Rose, C.W., Hairsine, P.B., (1988). "Flow and Transport in the Natural Environment: Advances and Applications." In: *Process of water erosion*, Steffen, W.L., Denmead, O. T. (eds.). Springer Verlag, Berlin, pp. 312-326.

Rose, C.W., Williams, J.R., Sander, G.C. and

Barry, D.A. (1983a). "A mathematical model of soil erosion and deposition processes, I. Theory for a plane land element." *Soil Sci. Soc. Am. J.*, Vol. 47, pp. 991-995.

Rose, C.W., Williams, J.R., Sander, G.C. and Barry, D.A., (1983b). "A mathematical model of soil erosion and deposition processes, II. Application to data from an arid-zone catchment." *Soil Sci. Soc. Am. J.*, Vol. 47, pp. 996-1000.

Rose, C.W. Hairsine, P.B., Proffitt, A.P.B. and Misra, R.K. (1990). "Interpreting the role of soil strength in erosion processes." *Catena Supplement*, Vol. 17, pp. 153-165.

Rose, C.W. (1993). "Hydrology and water management in the humid tropics - Hydrological research issues and strategies for water management." In: *Erosion and sedimentation*, Bonnell, M., Hufschmidt, M.M., Gladwell, J.S. (eds.), Cambridge University Press, Cambridge, UK, pp.301-343.

Siepel, A.C. (1994). *Re-entrainment and settling velocity in a physically-based erosion model.* presented to the Honors Committee in the Physical Sciences of the College of Agriculture and Life Sciences, Cornell University, Ithaca, NY.

Sloan, P.G. and Moore, I.D. (1984). "Modeling subsurface stormflow on steeply sloping forested watersheds." *Water Resour. Res.*, Vol. 20, pp. 1815-1822.

U.S. Army CERL. (1993). *GRASS 4.1 User's Manual.*, Construction Engineering Research Laboratory, Champaign, IL.

Zollweg, J.A. (1994). Effective use of Geographic Information Systems for rainfall-runoff modeling. PhD Thesis, Cornell University, Ithaca, NY.

Seong-Joon Kim, #1 Hwayang-dong, Gwangjin-gu, Seoul 143-701, Korea
(E-mail:kimsj@konkuk.ac.kr)

(Received December 7, 2000; accepted February 7, 2001)